Bio-Inspired Navigation of Chemical Plumes

Maynard J. Porter III, Captain, USAF
Department of Electrical and Computer Engineering
Air Force Institute of Technology
Dayton, OH 45433-7765, U.S.A.
maynard.porter@afit.edu

Juan R. Vasquez, Lieutenant Colonel, USAF
Assistant Professor
Department of Electrical and Computer Engineering
Air Force Institute of Technology
Dayton, OH 45433-7765, U.S.A.
juan.vasquez@afit.edu

Abstract - *The ability of many insects, especially moths, to locate either food or a member of the opposite sex is an amazing achievement. There are numerous scenarios where having this ability embedded into ground-based or aerial vehicles would be invaluable. This paper presents results from a 3-D computer simulation of an Unmanned Aerial Vehicle (UAV) autonomously tracking a chemical plume to its source. The simulation study includes a simulated dynamic chemical plume, 6-degree of freedom, nonlinear aircraft model, and a bio-inspired navigation algorithm. The emphasis of this paper is the development and analysis of the navigation algorithm. The foundation of this algorithm is a fuzzy controller designed to categorize where in the plume the aircraft is located: coming into the plume, in the plume, exiting the plume, or out of the plume.*

Keywords: Fuzzy logic, plume tracking, navigation, plume navigation, bio-inspired.

1 Introduction

The research discussed herein is a key stepping stone in the development of a navigation algorithm to aid an unmanned aerial vehicle in tracking a chemical/odor plume to its source. The navigation algorithm developed was inspired by the abilities of the male Tobacco Hornworm moth (Manduca Sexta). The male Manduca Sexta (M.Sexta) has been widely studied regarding its ability to locate a female, via the female's pheromone plume, through turbulent air flow. This purely instinctual ability allows the moth to successfully navigate a plume to its source on the first try, strongly emphasizing that learning is unlikely to be a factor in M.Sexta's capability of navigating a pheromone plume [1][2]. If within nature there exists animals with the ability to successfully track chemical/odor plumes, attempting to reverse-engineer these techniques seems a viable solution to the plume tracking problem.

The typical structure of a M.Sexta's flight profile while tracking a plume begins with the initial pheromone contact. Upon such contact, the male moth who is likely downwind from the pheromone source, will immediately maneuver into the wind and begin an upwind movement [3]. Figure 1 illustrates the flight profile exhibited during its upwind, pheromone tracking behavior. The moth's pheromone tracking consists of three main behaviors: Casting; Counterturning; and Surging. Casting occurs when the insect has lost contact with the pheromone plume. The moth's speed increases and it flies perpendicular to the direction of the wind, increasing its chances of once again detecting the pheromone. Counterturning is an "in the plume" behavior as the moth moves in a zigzag pattern while maintaining upwind progress. Surging is a more narrower version of Counterturning, occurring as the moth detects an increased concentration of pheromone. While making upwind progress, the moth makes a zigzag pattern across the direction of the wind [4]. However, the degree by which the moth travels across the wind can vary significantly. If the moth looses contact with the pheromone, the counterturning behavior will cover a larger crosswind area. This casting behavior results in larger crosswind movements with turns potentially increasing to 180°or more. Such behavior could lead to zero upwind, or even downwind displacement, as the moth tries to relocate the plume. Casting will continue until the moth either detects the pheromone again or it gives up [3]. When the moth detects higher concentrations of pheromone, its crosswind movement decreases, resulting in a surge to the source [3].

Over the last 20 years, there have been several

Report Documentation Page

Form Approved
OMB No. 0704-0188

1. REPORT DATE	2. REPORT TYPE	3. DATES COVERED
JUL 2006		**00-00-2006 to 00-00-2006**

4. TITLE AND SUBTITLE	5a. CONTRACT NUMBER
Bio-Inspired Navigation of Chemical Plumes	5b. GRANT NUMBER
	5c. PROGRAM ELEMENT NUMBER
6. AUTHOR(S)	5d. PROJECT NUMBER
	5e. TASK NUMBER
	5f. WORK UNIT NUMBER
7. PERFORMING ORGANIZATION NAME(S) AND ADDRESS(ES) **Air Force Institute of Technology,Department of Electrical and Computer Engineering,Dayton,OH,45433-7765**	8. PERFORMING ORGANIZATION REPORT NUMBER
9. SPONSORING/MONITORING AGENCY NAME(S) AND ADDRESS(ES)	10. SPONSOR/MONITOR'S ACRONYM(S)
	11. SPONSOR/MONITOR'S REPORT NUMBER(S)

12. DISTRIBUTION/AVAILABILITY STATEMENT
Approved for public release; distribution unlimited

13. SUPPLEMENTARY NOTES
9th International Conference on Information Fusion, 10-13 July 2006, Florence, Italy. Sponsored by the International Society of Information Fusion (ISIF), Aerospace & Electronic Systems Society (AES), IEEE, ONR, ONR Global, Selex - Sistemi Integrati, Finmeccanica, BAE Systems, TNO, AFOSR's European Office of Aerospace Research and Development, and the NATO Undersea Research Centre.

14. ABSTRACT
see report

15. SUBJECT TERMS

16. SECURITY CLASSIFICATION OF:			17. LIMITATION OF ABSTRACT	18. NUMBER OF PAGES	19a. NAME OF RESPONSIBLE PERSON
a. REPORT **unclassified**	b. ABSTRACT **unclassified**	c. THIS PAGE **unclassified**	**Same as Report (SAR)**	**8**	

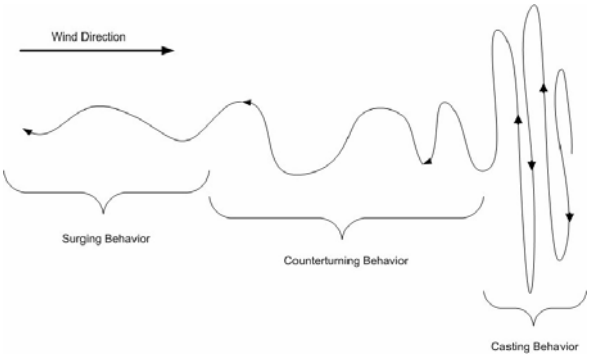

Figure 1: MSexta's flight profile

attempts to develop navigation schemes based on M.Sexta's abilities as well as similar abilities among other animals and insects. Farrell et al. [5] have developed the most advanced and thorough 2-D robotic implementation of an odor-based navigation system. The primary inspirations behind the algorithms used were taken from the behaviors of both moths and Antarctic procellariiform seabirds [5][6]. The authors' goals were to navigate and locate the source of an underwater chemical plume (Rhodamine dye) using an Autonomous Under Water Vehicle (AUV) located in a turbulent, near-shore, ocean environment. A flowchart of the navigation algorithm is shown in Figure 2, where d = detection, $\bar{d}$ = no detection, S = source declared, and $\bar{S}$ = source not declared. For the Reacquire behavior, the AUV conducts a maneuver depicted in Figure 3. A more thorough discussion of this algorithm can be found in [5].

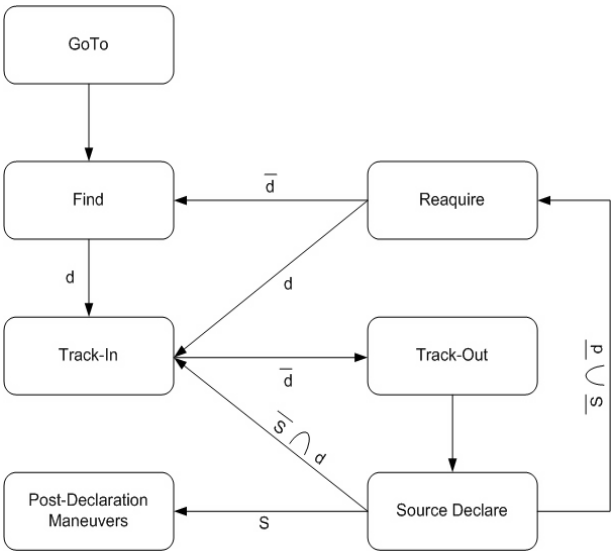

Figure 2: Farrell et. al. 2-D algorithm flow chart

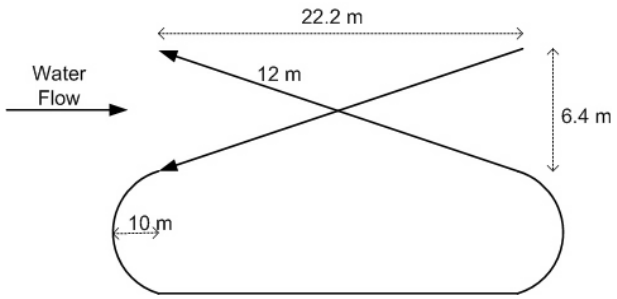

Figure 3: Bowtie maneuver

2 Simulation development

2.1 Plume model

The creation of a realistic plume model is important to the validity of the navigation algorithm which is developed based on the plume model. However, the use of a very accurate plume model can be extremely computationally expensive. One of the goals of this research was to have the simulation run in a matter of hours. Hence, a low fidelity plume model was used to satisfy computation limitations.

The plume model generates a new particle every second and propagates each particle independently through a modified biased random walk process. An initial plume is generated from 10,000 particles that can then be propagated over time via the biased random walk process. One example of an initial plume is illustrated in Figure 4 with final plume shown in Figure 5. The simulation takes approximately 45 minutes to complete, and the initial plume used to start the simulation takes fewer than 20 minutes to generate.

Concentration was ignored in the development of the plume for two reasons:

1. Decreased computation time by not dealing with calculating the diffusion of each particle.

2. Most computer simulations and robotic implementations incorporate a binary sensor, neglecting the need for generating concentration information in the plume model.

2.2 Dynamics model

The UAV dynamics model used for this research was developed from a 6-degree of freedom, non-linear, F-16 dynamics model. The F-16 model is a validated aircraft model [7] which is derived in detail in [8]. The F-16 model was scaled down to meet the capabilities of a small UAV and is provided in [13]. This UAV dynamics model met the needs of the simulation by maintaining stable flight for:

- Velocities: 10 $\frac{\text{ft}}{\text{s}} \rightarrow 35 \ \frac{\text{ft}}{\text{s}}$
- Altitudes: 0 ft $\rightarrow$ 3,000 ft

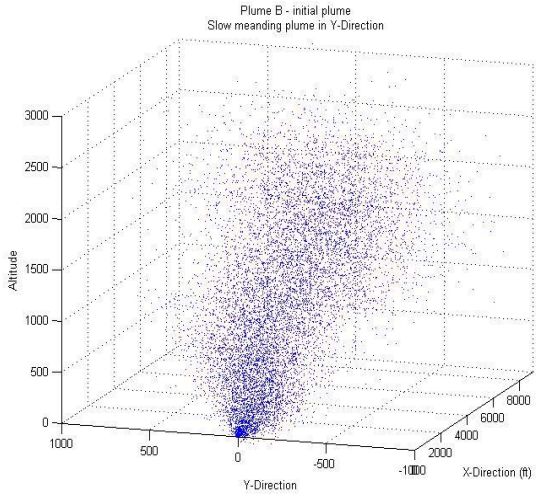

Figure 4: Initial 3-D plume

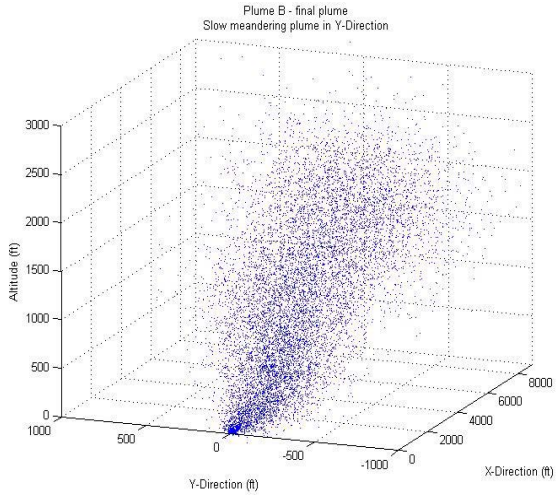

Figure 5: Final 3-D plume

Given the inputs available to the dynamics model, three autopilot control loops were used to pilot the UAV: altitude hold, velocity hold, and heading hold. Therefore, the navigation algorithm was designed to output a desired altitude (h), velocity (V_{uav}) and heading (ψ_{uav}). A diagram depicting the autopilot program is given in Figure 6. The methodologies behind how the autopilot maintains a commanded h, V_{uav}, and ψ_{uav} are given in [13].

2.3 Sensor model

The sensor model used in the simulation is of a simple design. If a plume particle falls within a set distance (defined by the user) of the UAV, then a detection is made. As the dynamic plume models used by the simulation do not incorporate concentration, the detection is purely binary. This has been a common practice used in most odor-based navigation simulations in the open literature [1][5][9][10][11][12]. Due to the inaccuracies of the plume model, changing the size of the sensor is a reflection of the plume density rather than

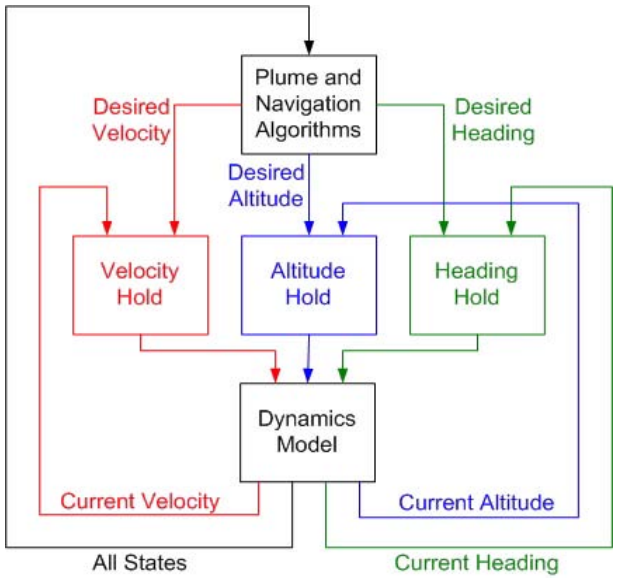

Figure 6: Autopilot flowchart

the sensitivity of the sensor. The sampling rate of the sensor is 10 Hz. Once the sensor information is passed into the navigation algorithm, a new maneuver may be generated.

2.4 Navigation algorithm

The UAV navigation algorithm consists of four tracking/search schemes: Tracking, Horizontal Search, Backtrack, and Vertical Search. These routines were developed from a mix of bio-inspiration and ad hoc engineering approaches. The Tracking scheme is based on a short term memory (STM) algorithm which is unique to this research. The Horizontal Search scheme is directly inspired by the moth's casting behavior. Backtrack is a method of relocating the plume, once the UAV is thought to be lost, by returning to the vicinity of the last detection. This methodology was adapted from the 2-D robotic simulation found in [5]. The Vertical Search scheme is unique to this research and was developed using ad hoc engineering approaches. An important parameter for the navigation algorithm as a whole is the time since last detection, T_D. Setting a threshold, ζ, for T_D dictates how long the UAV will stay in the Horizontal Search Routine before switching to the Backtrack Routine. Figure 7 illustrates how these tracking routines are intertwined, forming the complete navigation algorithm.

Tracking algorithm Figure 8 illustrates the STM. The length of the STM was set to 10 s, consisting of sensor data collected at 10 Hz (i.e., 100 memory locations). The position of the UAV, relative to the plume, is found by taking the mean of the locations in memory where detections occurred.

1. Average of $1 \rightarrow 40$, UAV is entering the plume
2. Average of $30 \rightarrow 80$, UAV is in the plume

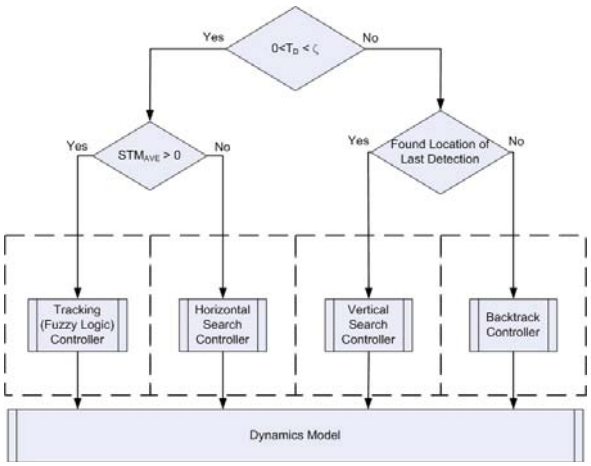

Figure 7: High-level navigation flowchart

3. Average of 60 → 100, UAV is leaving the plume

4. Average of 0 → UAV is out of the plume

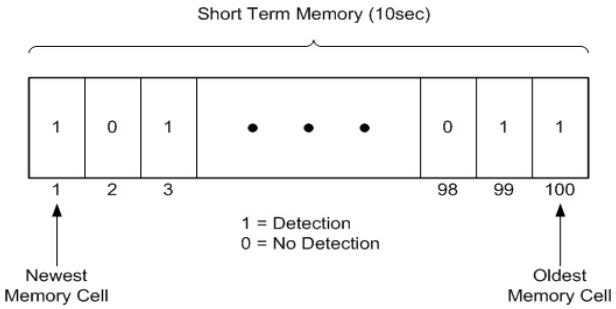

Figure 8: Short term memory

The UAV will use this tracking algorithm as long as detections exist in the STM. Due to the ambiguity in the UAV's location relative to the plume, it is pragmatic to use a fuzzy controller to generate the maneuver decision. The fuzziness of the STM is described by the overlap between the membership functions of the STM fuzzy set, as seen in Figure 9. This is used in concert with the time since the UAV crossed the wind line, T_Z, in order to help the UAV stay within the plume.

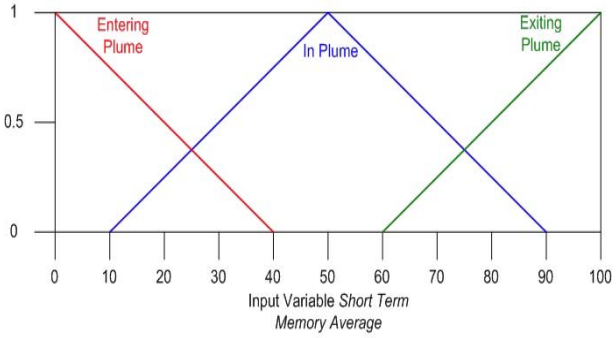

Figure 9: Short term memory fuzzy set

After the new heading is calculated from the STM and T_Z, a delta-heading is found. This delta-heading represents how many degrees the UAV must turn, and is used to calculate a new velocity. The new velocity is found using a fuzzy controller with delta-heading as the input and velocity as the output. The velocity fuzzy controller is depicted in Figure 10. In order to make a sharp turn, the aircraft has to decrease its velocity. This allows for a tighter turn without pulling an excessive amount of g's.

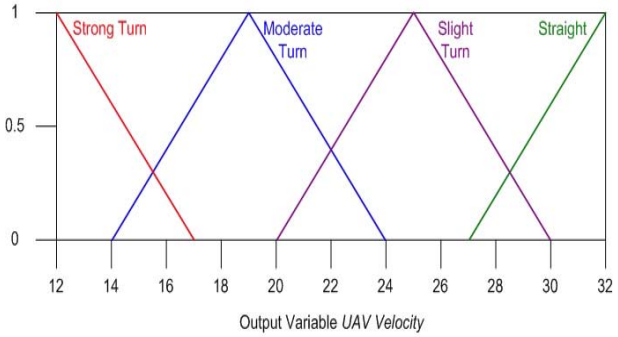

Figure 10: Velocity fuzzy set

Horizontal search routine The Horizontal Search routine is implemented for a given length of time, ζ, beginning from the time when zero detections occur in the STM. During this routine, the UAV will maintain altitude while conducting a casting type of maneuver perpendicular to the wind. This maneuver is illustrated in Figure 11. The UAV will continually increase the distance traveled across the wind line by increasing the time between counterturns, T_{ct}, by ΔT_{ct}.

This search routine will be terminated when either the UAV makes a detection, or ζ is exceeded. If a detection is made, the Tracking routine will be executed, and if ζ is reached before a detection occurs, the Backtrack routine will be executed.

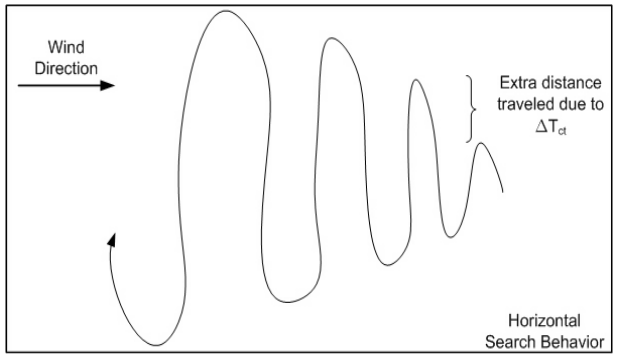

Figure 11: Illustration of the Horizontal Search routine

Backtrack routine This routine is executed when the UAV has lost the plume. Farrell et al. [5] used a method in their 2-D robotics navigation algorithm that guided the robot back to the position where it

last made a detection. This method worked quite well in their 2-D experiments, and was used as the basis for the Backtrack routine. The UAV is assumed to have GPS capabilities on board and has the ability to store the location of the last detection in memory. When the Backtrack routine is executed, the UAV returns to within a certain radius, r_{BT}, of the same horizontal location of the last detection. However, the altitude is decreased by Δh, which is varied with altitude. Table 1 gives the range of values for Δh.

Table 1: Varying altitude changes for Backtrack routine

Current Altitude (ft)	Δh
$600 \leq h$	100
$200 \leq h < 600$	50
$50 \leq h < 200$	25
$h < 50$	10

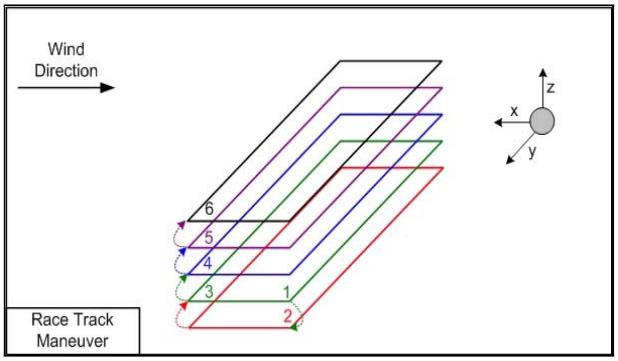

Figure 12: Illustration of Vertical Search routine

Table 2: Table of scenarios for UAV simulation study

$\Delta T_{ct} \backslash \zeta$	180	240	300	420
10	x	x	N/A	N/A
20	x	x	x	x
30	N/A	x	N/A	N/A

Vertical search routine The bulk of the UAV's movement up to this point has taken place in the horizontal plane, with little change in altitude. The assumption is that the mean wind direction will not change drastically over a short period of time (10's of minutes). The plume should still be in the same vicinity as it was during the last detection. Therefore, searching the horizontal plane over varying altitudes should result in a detection. The routine begins by traveling in a race track pattern at the altitude the UAV was flown to by the Backtrack routine, but Δh below the altitude of the last detection. The rational for decreasing the altitude by Δh is tied to the assumption that the UAV exited the plume from above, as would typically be the case for a rising plume. Once this pattern is complete, the UAV decreases in altitude another Δh, executing the racetrack flight profile again. The racetrack profile is executed 4 more times, except instead of decreasing in altitude, the UAV increases its altitude each time by Δh. A detailed illustration of this routine is shown in Figure 12.

Whenever a detection is made, this routine is terminated and the Tracking routine begins. If all six race tracks are completed without a detection, the UAV is declared lost and the simulation ends. This routine could have implimented additional memory to keep track of more than one detection location. However, in order to keep the simulation time to within a reasonable limit (5 hours) this limitation was imposed.

3 Sensitivity Analysis

3.1 Preliminary analysis

A sensitivity analysis of the navigation algorithm was performed in an attempt to maximize the UAV's success of reaching within 100 ft of the source, while also trying to minimize flight time. However, the main goal was to reach the source in the 7,000 s time frame allotted. The variables altered in the analysis were ζ and ΔT_{ct} as shown in Table 2. Each cell of Table 2 which contains an "x" represents one scenario tested, and the cells with "N/A" correspond to scenarios not tested. The reasoning behind not testing certain scenarios were time constraints and initial unsuccessful runs when incorporating larger values of ζ. A single simulation consists of 10 Monte Carlo runs of one scenario. Each of these simulations used sensor A (Sensor A = 25 ft, Sensor B = 40 ft radius) and was tested against one of four possible plume structures. The four plume types used are:

- Plume B: Slowly meandering plume that continually rises
- Plume C: Quickly meandering plume that continually rises
- Plume D: Slowly meandering plume that begins at an altitude of 500 ft and decreases slightly in altitude
- Plume E: Quickly meandering plume that begins at an altitude of 500 ft and decreases slightly in altitude

Figure 13 illustrates the number of successful runs for each scenario tested against Plume B using Sensor A. It is easy to see that ζ's of 180 s and 240 s have the highest success rate, as was also the case when tested against Plume C. To gather more insight, Figure 14 was created, comparing the means and standard deviation of the time taken to reach the source for successful runs. A ζ value of 180 s paired with a ΔT_{ct} of 10 had the largest standard deviation, however, it's performance overall was better than any other scenario. Figures 15 through 17 are plots of the trajectory of a successful UAV simulation (ζ = 180 s and ΔT_{ct} = 10 s) and associated plume. The different colors of the

trajectory represent which one of the four navigation routines the aircraft was operating in at that instant in time: Green = Tracking, Blue = Horizontal Search, Black = Backtrack, and Red = Vertical Search.

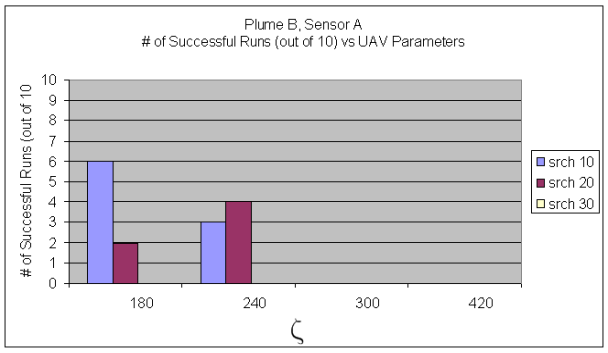

Figure 13: Plume B, Sensor A - Number of successes given 10 Monte Carlo runs of each scenario

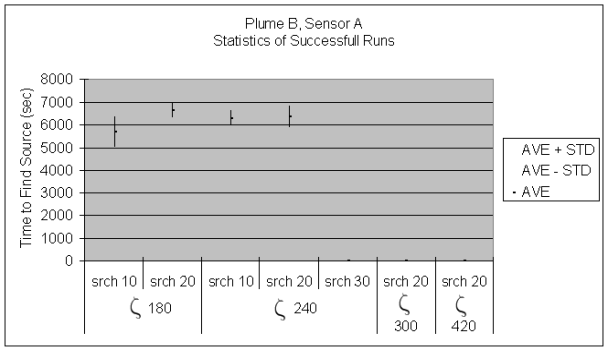

Figure 14: Plume B, Sensor A - Statistics for the time to source for successful Monte Carlo runs

When the scenarios given in Table 2 were tested against Plumes D and E (non rising plumes), the results were slightly different than with the previous plumes. However, the more successful ζ values were still 180 s and 240 s. The results from tests against Plume D are given in Figure 18. The statistics of the times associated with the successful runs against Plume D are illustrated in Figure 19. The results show the UAV is typically less successful for ζ values of 180 and 240 but more successful for values of 300 and 400. This is due to Plume D's structure and the Backtrack routine being designed more for a rising plume than a flat or descending plume.

3.2 Additional analysis

Taking the two best performing ζ values (180 s and 240 s), an additional scenario matrix was designed and is given in Table 3. This time, only two values were used for ΔT_{ct} (10 s and 20 s). However, two versions of the Backtrack routine were used along with a comparison of sensors A and B. The two versions of the Backtrack routine used were the original and one that was modified to command the UAV to go back to the exact

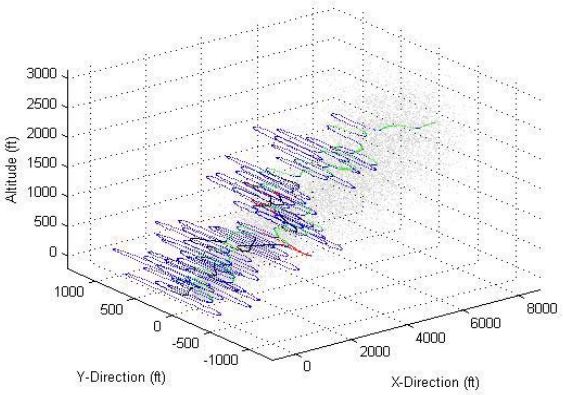

Figure 15: 3-D Plot of a successful run - plume B, sensor A, $\zeta = 180\,\text{s}$ and $\Delta T_{ct} = 10\,\text{s}$

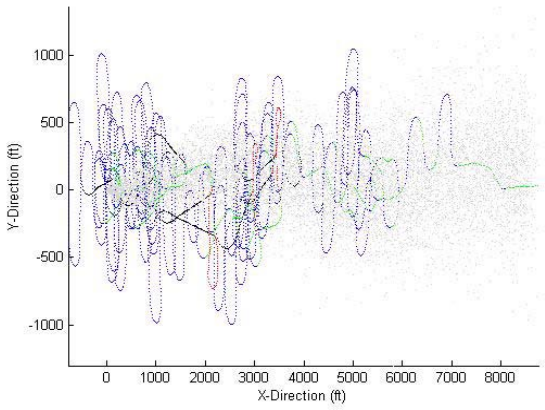

Figure 16: Horizontal plane of a successful run - plume B, sensor A, $\zeta = 180\,\text{s}$ and $\Delta T_{ct} = 10\,\text{s}$

location of the last detection (not below it). As expected the results for plumes B and C improved with the use of sensor B. However, the UAV never reached the source under the time limit when the new Backtrack routine was used due to more time spent in the Vertical Search routine. The results for plumes D and E improved slightly with sensor B and had negligible improvement with the new Backtrack routine. This lack of improvement given the new backtrack routine for against plumes D and E was not surprising. Since the aircraft typically flew below the plume, returning to the exact location of the last detection places the UAV at the bottom edge of the plume. This does not afford the aircraft the opportunity to begin its tracking routine in the center of the plume, increasing its chances of again flying out of the plume. The results for plume D are given in Figures 20 and 21.

4 Conclusion

The cornerstone of the navigation algorithm is the Tracking routine. The idea of using memory to help make a maneuver decision is unique to this research, as

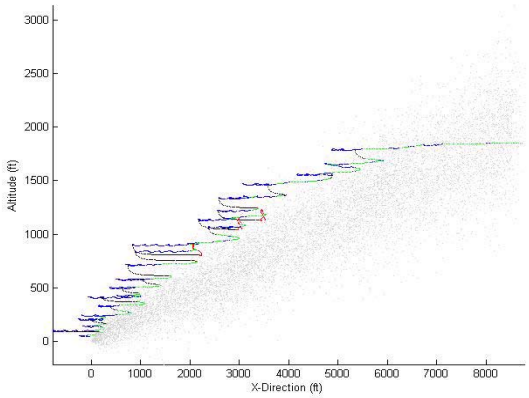

Figure 17: Vertical plane of a successful run - plume B, sensor A, $\zeta = 180\,\mathrm{s}$ and $\Delta T_{ct} = 10\,\mathrm{s}$

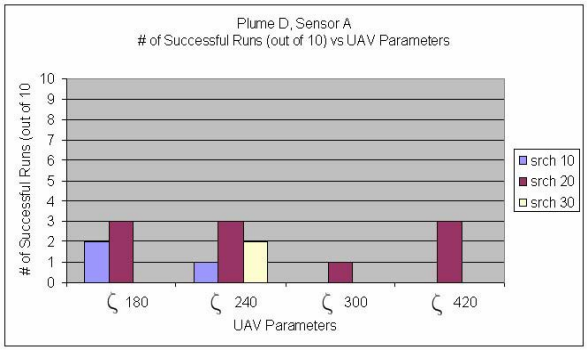

Figure 18: Plume D, Sensor A - Number of successes given 10 Monte Carlo runs of each scenario

prior research efforts made maneuver decisions based on single detections. The success rate of up to 70% given the 7,000 s time frame is a notable achievement for the first set of experiments. Obviously, taking almost 6 hours to traverse a 9,000 ft plume is not optimal, but this is a step in the right direction. Given the results in Section 3, two potential improvements are:

1. Decreasing ζ: This will make the UAV spend less time in the Horizontal Search algorithm (the most used algorithm), executing the Backtrack routine quicker. This will return the UAV back to the plume, spending less time searching when it is out of the plume.

2. Helical flight pattern: The M.Sexta data suggest that the optimal 2-D search pattern has a sinusoidal nature. Extending this to 3-D brings the thought of a helical flight path, searching the horizontal plane as well as the vertical plane.

Table 3: Additional scenarios for UAV simulation study (Btk = Backtrack)

ΔT_{ct} \	$\zeta = 180$				$\zeta = 240$			
	Sensor A		Sensor B		Sensor A		Sensor B	
	Orig Btk	New Btk	Orig Btk	New Btk	Orig Btk	New Btk	Orig Btk	New Btk
10	x	x	x	x	x	x	x	x
20	x	x	x	x	x	x	x	x

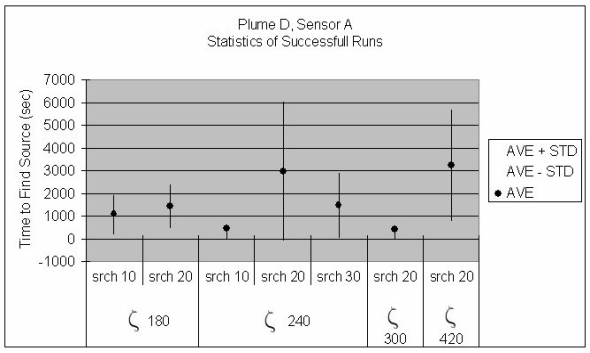

Figure 19: Plume D, Sensor A - Statistics for the time to source for successful Monte Carlo runs

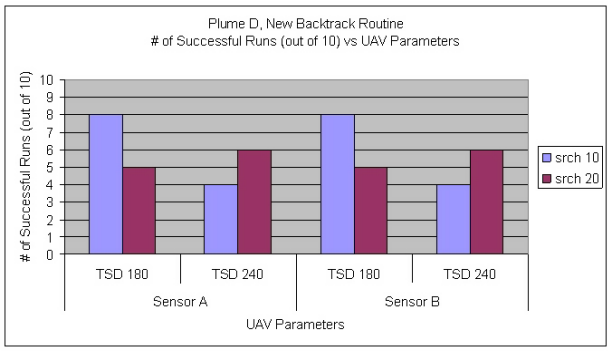

Figure 20: Plume D, Sensor A with new Backtrack routine - Number of successes given 10 Monte Carlo runs of each scenario

The success of this research lays the foundation for developing the odor-based navigation algorithms of small UAV's owned and operated by the Air Force Research Lab, Sensor's Directorate, at Wright Patterson Air Force Base.

References

[1] J. H. Belanger and E. A. Arbas. "Behavioral strategies underlying pheromone modulated flight in moths: lessons from simulation studies". *Journal Comp Physiol*, A:345–360, 1998.

[2] M. A. Willis and E. A. Arbas. "Odor-modulated upwind flight of the sphinx moth, Manduca Sexta". *Journal Comp Physiol*, A:427–440, 1991.

[3] E. A. Arbas, M. A. Willis and R. Kanzaki. *Organization of goal-oriented locomotion: pheromone-modulated flight behavior of moths,* volume Biological Neural Networks in Invertebrate Neuroethology and Robotics of Neural Networks: Foundations to Applications, chapter 8, 159-198, Harcourt Brace Jovanovich, 1993.

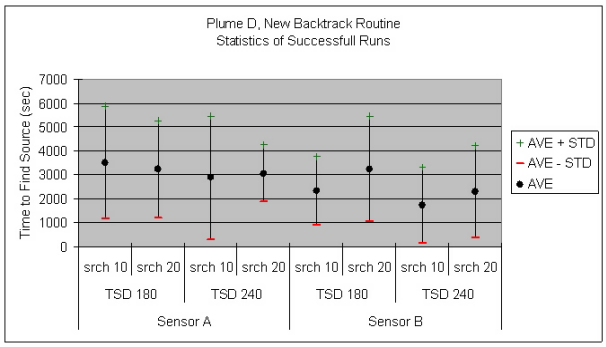

Figure 21: Plume D, Sensor A with new Backtrack routine - Statistics for the time to source for successful Monte Carlo runs

[4] J. S. Kennedy. *Olfactory Responses to distant plants and other odor sources,* 67-91. Shorey H.H., and McKelvey J.J. Wiley-Interscience, New York, 1977.

[5] J. A. Farrell, S. Pang and W. Li. "Chemical plume tracing via an autonomous underwater vehicle". *IEEE Journal of Ocean Engineering*, 30(2):428–442, 2005.

[6] G. A. Nevitt. "Olfactory foraging by antartic procellariiform seabirds: life at high reynolds numbers". *Biological Bulletin*, 198:245–253, Apr 2000.

[7] B. S. Liebst and C. H. Spenny. Nonlinear Dynamic Model of the F-16 Aircraft, 2000.

[8] B. L. Stevens and F. L. Lewis. *Aircraft Control and Simulation*, John Wiley and Sons Inc., 1992.

[9] L. Marques, U. Nunes and A. T. Almeida. "Olfaction-based mobile robot navigation". *Thin Solid Films*, 418:51–58, 2002.

[10] R. Vabo, G. Huse, A. Ferno, T. Jorgenson, S. Lokkeborg and G. Skaret. "Simulating search behaviour of fish towards bait". *ICES Journal of Marine Science*, 61:1224–1232, 2004.

[11] H. Ishida, G. Nakayama, T. Nakamoto and T. Moriizumi. "Controlling a gas/odor plume-tracking robot based on transient responses of gas sensors". *IEEE Sensors Journal*, 5(3):537–545, Jun 2005.

[12] W. Li, J. A. Farrell and R. T. Cardé. "Tracking of fluid-advected odor plumes: strategies inspired by insect orientation to pheromone". *Adaptive Behavior*, 9(3-4):143–170, 2001.

[13] M. J. Porter. *Bio-Inspired Odor-Based Navigation.* M.S. thesis, Air Force Institute of Technology, 2006.